The Chemist
Journal of the American Institute of Chemists

Microenvironment-sensitive Fluorophore for Recognition of Human Serum Albumin in Aqueous Solution

Rajib Choudhury*, Siddhi R. Patel, Hannah R. Lykins
Department of Physical Sciences, Arkansas Tech University, Russellville, Arkansas, 72801, United States
*(*E-mail: rchoudhury@atu.edu)*

Abstract: In this work, the efficacy of a donor-acceptor based red light emitting fluorophore has been assessed for human serum albumin (HSA) detection in aqueous samples. Due to intramolecular charge transfer (ICT) within an extended π-conjugated framework and the positive solvatochromic property, the fluorophore emitted in the far-red region of the electromagnetic spectrum in aqueous buffer samples. The fluorescence intensity was highly sensitive to the microenvironment, which resulted strong turn-on fluorescence response upon encapsulation of the fluorophore within the HSA. The signal was quantitative to the amount of fluorophore-protein complex in the experimental concentration range. The strong association affinity of the fluorophore toward HSA was attributed to the van der Waals and hydrophobic interactions. Such a spontaneous supramolecular association and the subsequent turn-on fluorescence response has potential for medical diagnostic applications.

Key Words: Fluorophore, microenvironment, human serum albumin

INTRODUCTION

Human serum albumin (HSA) is the most abundant protein in blood plasma [1]. It maintains the osmotic pressure of the blood compartment and transports both exogenous and endogenous ligands to various sites [2-4]. It is an important biomarker as different amounts of HSA in body fluids indicate different health conditions, including kidney and cardiovascular damage [5-7]. Therefore, a great amount of resources has been devoted to sensing and the detection of HSA in biological samples. Several techniques such as immunoassay, radioimmunoassay, capillary electrophoresis, spectrometric and fluorimetric techniques, etc., are currently available [8-14]. Among these techniques, the fluorimetric method has attracted much attention recently since it is quick, cost-effective, non-invasive and very accurate [15-17]. Fluorimetric techniques measure the alteration of the emission profile of the fluorophore upon interaction with HSA. If the change of fluorescence signal is significant and correlates with the quantitative amount of protein-fluorophore complex, then a simple fluorophore based sensor can be developed. But, a suitable fluorophore is always required which would undergo photophysical property change in the presence of HSA and emit light as output signal detectable by standard fluorimeters.

Therefore, an upsurge in the quest for suitable fluorophores for "turn-on" HSA sensors has been noticed. In this regard, environmentally sensitive fluorophores are very promising as their emission intensity significantly changes upon encapsulation within a biomolecule [18-20]. The rigid environment and multiple non-covalent forces reduce the degrees of freedom of the encapsulated fluorophore, hindering non-radiative energy loss and hence increase in fluorescence intensity [18]. The hydrophobic effect also plays a major role in the protein-fluorophore supramolecular complexation and the associated fluorescence enhancement [21]. Lipophilic ligands bind within the HSA's pockets by hydrophobic interactions. As the lipophilicity increases binding affinity increases and the lifetime of the fluorescence lengthens. However, a highly lipophilic compound tends to aggregate heavily in water [22]. If aggregate interactions are stronger than the protein-fluorophore interactions, then the fluorophore becomes unsuitable for the HSA sensing application. Therefore, the fluorophore must remain soluble to some extent in water or at least it should not form strongly clustered aggregates.

Herein, we have studied one such environmentally sensitive fluorophore for HSA detection in aqueous buffer samples. A nitrogen donor and three nitrile acceptors are connected by an extended π-conjugation (Figure 1c). The fluorophore emits in the far-red region of the spectrum, indicating the potential for applications with biological samples since it would be free from background emission of other biomolecules [23-24]. It consists of two –OH groups which deliver the required solubility for applications in aqueous solution.

EXPERIMENTAL

All the reagents were purchased from commercial vendors (Millipore Sigma and Alfa Aesar) and used without further purification. All the solvents were of the spectrophotometric grade. Water was purified using a deionization system.

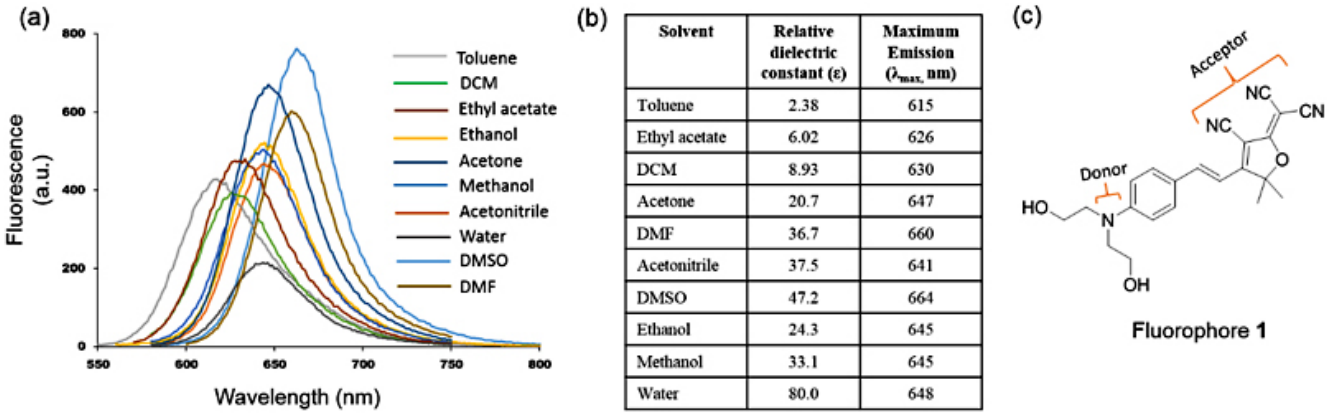

Solvent	Relative dielectric constant (ε)	Maximum Emission (λ_{max}, nm)
Toluene	2.38	615
Ethyl acetate	6.02	626
DCM	8.93	630
Acetone	20.7	647
DMF	36.7	660
Acetonitrile	37.5	641
DMSO	47.2	664
Ethanol	24.3	645
Methanol	33.1	645
Water	80.0	648

Fig 1. (a) Emission spectra of 1 in various solvents. [1] = 1.0 × 10^{-5} M; aqueous solution contains 1% DMSO. (b) Positive solvatochromism of fluorophore 1 with polarity of solvents. (c) Structure of fluorophore 1

Absorption spectra were collected on a Shimadzu UV-2501 PC spectrophotometer. Emission spectra were obtained using an LS 55 Luminescence Spectrometer (PerkinElmer) with 5 nm excitation and emission slit widths and 200 nm/min scan speed. Molecular docking was performed on a single CPU Windows-OS computer (64-bit) with 3.30 GHz processor and 8.00 GB of RAM on Vina 1.1.2 program [25]. 3D coordinate structure of the fluorophore (Figure 1c) was constructed and optimized with an MM2 force field on Chem3D. Coordinates of the HSA were obtained from protein crystal structure (PDB code: 2BXC). AutoDock Tools 1.5.6 was used for the preparation of protein and fluorophore input files in pdbqt format, which is a modified protein data bank format containing atomic charges, atom type definitions and, for fluorophore, topological information. Gasteiger partial charges were added to the fluorophore; non-polar hydrogen atoms were merged, and torsional rotatable bonds were defined. All the single bonds were made rotatable; double and triple bonds were kept as non-rotatable. All other parameters were kept at their AutoDock default values. A rectangular box of dimensions 34 × 34 × 32 $Å^3$ with 1.0 A grid spacing was constructed to encompass the entire site I of HSA. The exhaustiveness of the docking run was set at 20 and the seed was varied randomly as generated by the program.

RESULTS & DISCUSSION

Fluorophore **1** is moderately soluble in water. It is highly soluble in acetone and in halogenated solvents such as chloroform and dichloromethane, as well as in polar aprotic solvents such as dimethyl sulfoxide (DMSO) and dimethylformamide (DMF). For all the spectrometric experiments a DMSO stock of **1** was diluted in 0.1 M phosphate buffer (pH = 7.5) solution. The final DMSO

content in buffer was 1%, and the concentration of **1** was maintained at 10 μM unless otherwise stated.

Fluorophore **1** exhibited strong fluorescence in DMSO, DMF, and acetone; moderate emission in nonpolar solvents such as toluene and ethyl acetate and very weak emission in deionized water (Figure 1a). All the emission bands were very broad and structureless, which is characteristic of donor-acceptor charge transfer type electronic transition. Emission intensity and position of the bands were very sensitive to the polarity of the solvents, indicating strong solvatochromism (Figure 1b) [26]. As the polarity of the solvents increased the emission maxima shifted toward lower energy, suggesting a positive solvatochromism [26]. The lowest energy charge transfer emission recorded was in DMSO (λ_{max}^{em} ~ 665 nm). In water emission maxima was at ~ 648 nm with the lowest intensity, most likely due to loss of excited state energy through additional decay channel facilitated by polar protic water through hydrogen bonds.

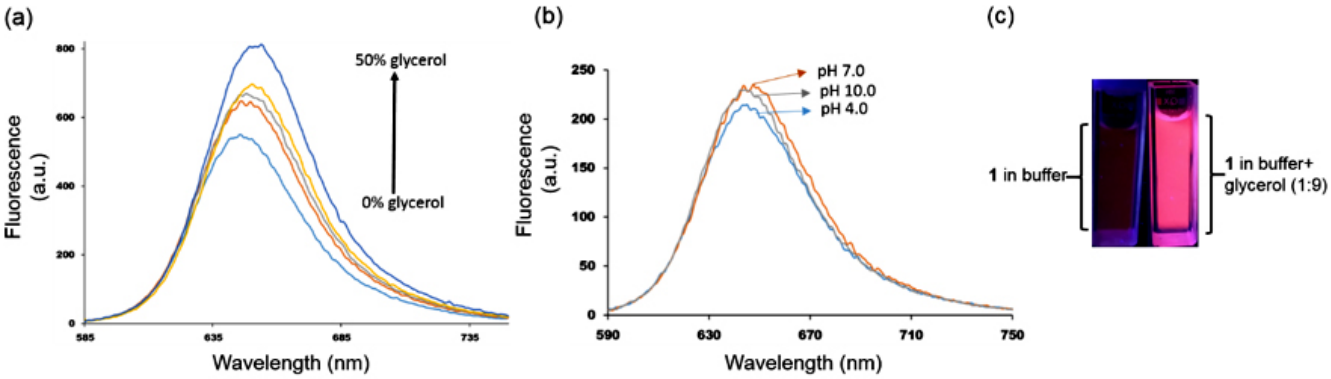

Fig 2. (a) Fluorescence of 1 with added glycerol in methanol. (b) Fluorescence of 1 at different pH values: 4.0, 7.0, and 10.0. (c) The appearance of bright red fluorescence in glycerol/buffer (9:1) mixture.

Studies have revealed that the extent of emission (quantum yield of fluorescence) of the flexible donor-acceptor fluorophores is dependent on the solvent polarity and the identity of the environment [18]. Excited state energy can dissipate via several non-radiative pathways, including rotation of the single bonds. Fluorophore **1** consists of several C-C and C-N single bonds on the main π-conjugated backbone. Therefore, it is not surprising that the fluorescence of **1** is low in low viscous solvents.

Figure 2a shows the effect of the addition of a highly viscous solvent (glycerol, viscosity 950 cP at 25°C) to the fluorescence intensity of the **1**. It showed a broad emission in methanol centered at ~ 645 nm. But, when 10% glycerol was added an increase in intensity was noticed along with the slight bathochromic shift of the peak. As the amount of glycerol was gradually increased −and thus the viscosity of the mixture − enhancement of emission intensity was noticed. At 50% methanol/glycerol mixture (v: v) an almost two times increase in intensity was recorded. Figure 2c shows the solution of **1** in phosphate buffer and in 9:1 glycerol-buffer (v: v) mixture under UV light. In the latter case, the strong bright red fluorescence of **1** was visible to the naked eyes. Thus both these experiments demonstrate the strong environment effect on the fluorescence of **1**. A heavily viscous microenvironment hinders rotation of the bonds and other local motions, impeding non-radiative decay of the excited state energy.

Therefore, it would be of great interest to study the photophysical property of **1** in the presence of HSA. When a fluorophore binds within a binding pocket of the HSA, it experiences a new microenvironment which is very different from the bulk solvent. Fluorescence intensity and lifetime of the fluorophore change to a significant extent due to the confined geometry of the fluorophore in the protein's pocket. Narrow sterically crowded space and van der Waals interactions restrain the non-radiative decay and significantly increase the fluorescence intensity.

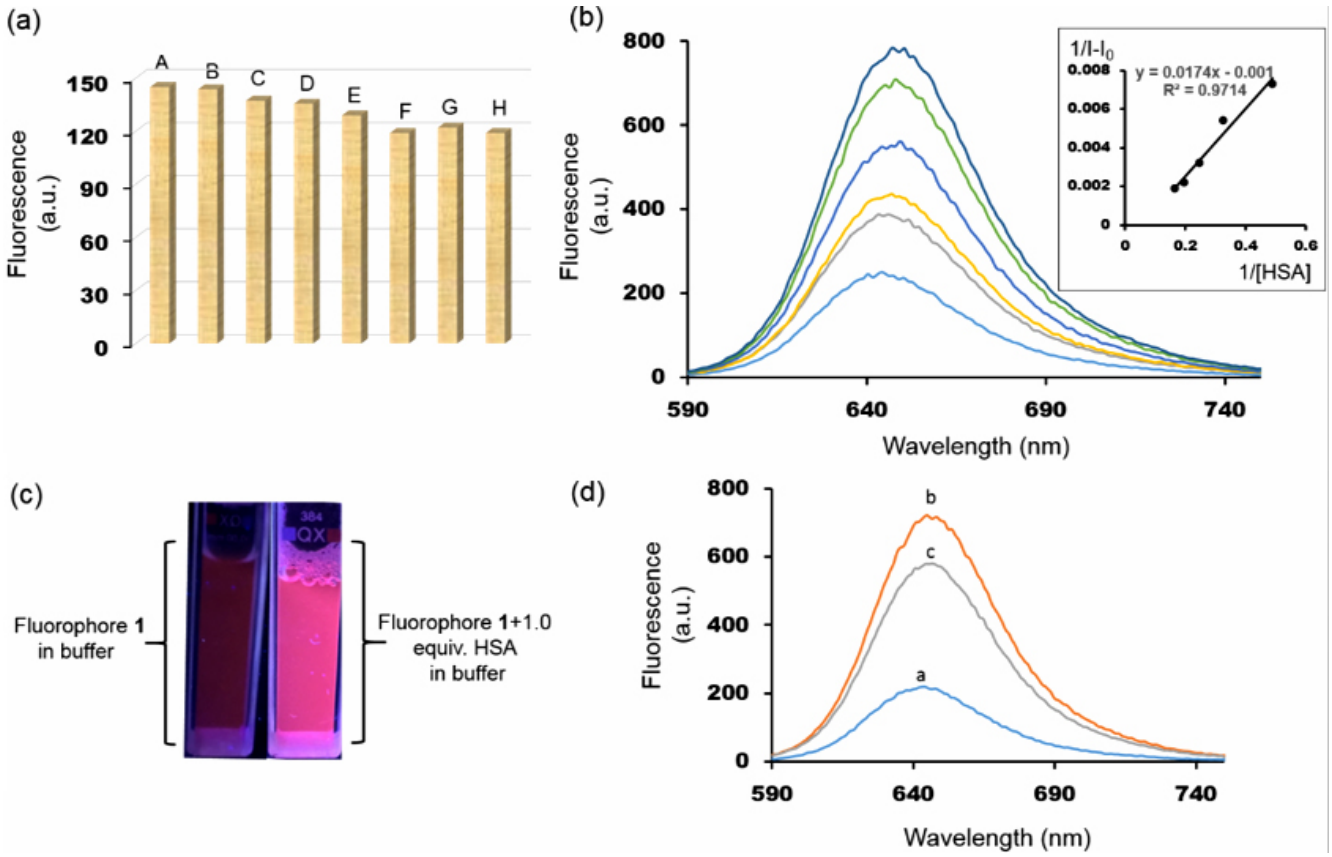

Fig 3. (a) (A) Fluorescence intensity of 1 in phosphate buffer, (B) in presence of Na^+ (1mM), (C) K^+ (1 mM), (D) NH_4^+ (1 mM), (E) Ca^{2+} (0.5 mM), (F) citric acid (1 mM), (G) lactic acid (1 mM), and (H) uric acid (1 mM). (b) Fluorescence spectra of 1 in presence of varying amount of HSA; [1] = 1.0 × 10^{-5} M. Inset: Benesi-Hildebrand plot of $1/[I-I_0]$ vs 1/[protein] (M^{-1}) for binding of 1 with HSA. (c) Appearance of red fluorescence upon addition of HSA, [HSA] = [1] = 10 μM. (d) Fluorescence spectra of 1 in presence of phenylbutazone in phosphate buffer. (a) Only 1 in buffer, (b) [1] = [HSA] = 10 μM, (c) [1] = [HSA] = [phenylbutazone] = 10 μM.

Since many properties and functions of biological macromolecules are dependent on the pH of the solution, we first studied fluorescence of **1** in a wide range of pH values. No change in emission intensity was noted from pH 4.0 to 10.0, indicating potential compatibility of **1** for biological applications (Figure 2b). Moreover, biological samples usually contain a large variety of cations such as Na^+, K^+, NH_4^+, Ca^{2+} and other molecules such as citric acid, lactic acid, uric acid, etc. Emission intensity of **1** was evaluated in the presence of these interfering ions and compounds. As shown in figure 3a, no significant change in emission was recorded in buffer solutions in the presence of the aforementioned ions and organic compounds. Next, to investigate the effect of HSA on the fluorescence of **1**, titration experiments were carried out in phosphate buffer solutions with 1% DMSO. Emission intensity increased upon addition of HSA. A linear relationship between concentrations of HSA and fluorescence intensity was observed, suggesting a 1:1 complex formation (Figure 3b).

From this relationship, the binding affinity (K_a) was calculated by using the Benesi-Hildebrand equation [27]. The K_a of **1** was found to be 5.75 ×10^4 M^{-1} (ΔG = -6.48 kcal/mol). It indicates a strong association of **1** with HSA guided by multiple weak non-covalent interactions and hydrophobic effect. Figure 3c shows the effect of the addition of one equivalent of HSA in a buffered solution of **1** under UV lamp. Negligible fluorescence now becomes visible to the naked eyes. The linear relationship between fluorescence intensity and added HSA and the dramatic increase in fluorescence intensity suggest that **1** can be used to detect HSA in biological samples.

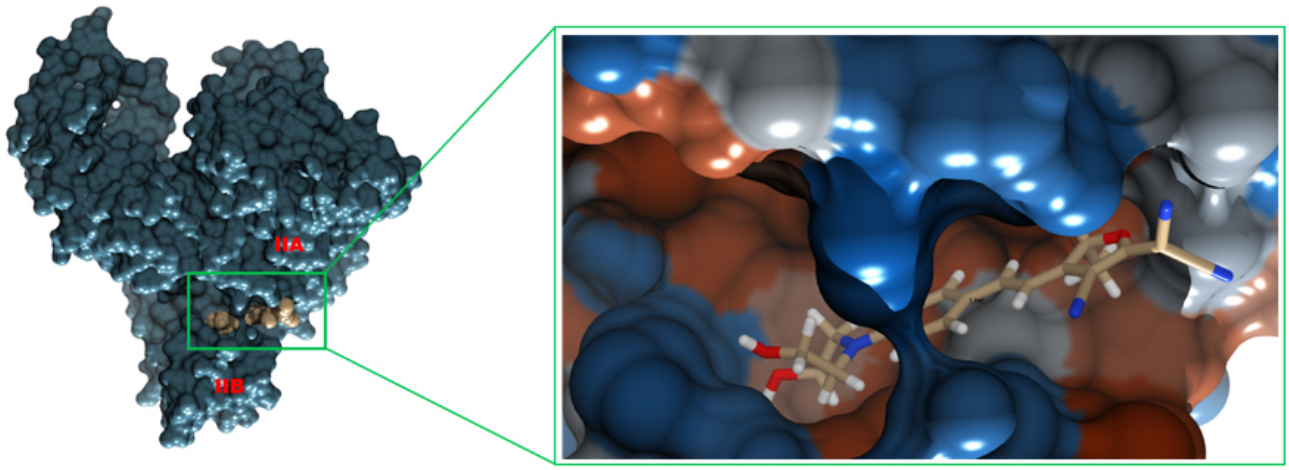

Fig 4. Docking conformation of the HSA-1 supramolecular complex with the lowest binding free energy.

Next, with the help of displacement assay and molecular docking, we investigated the fluorophore binding site in HSA. HSA has three ligand binding domains, and each domain is divided into two subdomains, subdomain A and subdomain B. The hydrophobic drug phenylbutazone binds within domain II (in subdomain IIA) with an affinity of 7.0×10^5 M^{-1}. Addition of equimolar amount of phenylbutazone into a 1:1 solution of HSA-**1** reduced the fluorescence intensity by ~20%, which indicates a competition between **1** and the drug for domain II (Figure 3d).

The molecular docking study between HSA and **1** provided additional information about the binding site of **1** in the HSA molecule. As shown in figure 4, **1** binds between the cavity of subdomain IIA and IIB, in one of the fatty acid binding sites [28]. The hydrophobic rings of **1** remain embedded within the deepest part of the cavity whereas the polar groups –OH and -CN are exposed to polar amino acids and water, respectively. Unlike phenylbutazone, **1** does not bind within subdomain IIA probably due to a larger size and polar nature of the functional groups.

CONCLUSIONS

In conclusion, an environmentally sensitive donor-π-acceptor based fluorophore has been assessed for HSA detection in aqueous buffer samples. The fluorophore showed positive solvatochromism. The fluorescence intensity was highly sensitive to the nature of the microenvironment. Upon binding with HSA the fluorescence intensity increased, displaying a "turn-on" fluorescence response.

Fluorescence response was quantitative for the HSA in aqueous buffer samples, demonstrating a potential for small molecule-based fluorescence sensor for HSA detection in biological samples. The fluorophore was insensitive to pH change and highly tolerant to common ions and organic molecules. It quickly formed a complex with HSA, settling within an area between subdomain IIA and IIB. The high binding affinity was presumably due to strong van der Waals and hydrophobic interactions. The turn-on fluorescence response can be further extended to the diagnosis of HSA protein in human urine samples and protein nanoparticle-based bioimaging.

ACKNOWLEDGMENTS

We would like to thank Arkansas Tech University's faculty research grant office for generous financial support.

Note: The authors declare no conflict of interest.

REFERENCES

1. Peters T in All About Albumin: Biochemistry, Genetics, and Medical Applications, Academic Press, San Diego, CA, 1996.
2. Ha CE, Bhagavan NV. *Biochim. Biophys. Acta*, 2013, 1830, 5486–5493.

3. Pal S, Saha C. *J. Biomol. Struct. Dyn*., 2014, 32, 1132−1147.
4. Fasano M, Curry S, Terreno E, Galliano M, Fanali G, Narciso P, Notari S, Ascenzi P. *IUBMB Life*, 2005, 57, 787−796.
5. Doumas BT, Peters T. *Clin. Chim. Acta,* 1997, 258, 3-20.
6. Arques S, Ambrosi P. *J. Card. Failure,* 2011, 17, 451-458.
7. Fanali G, di Masi A, Trezza V, Marino M, Fasano M, Ascenzi P. *Mol. Aspects Med*., 2012, 33, 209-290.
8. Thakkar H, Newman DJ, Holownia F, Davey CL, Wang CC, Lloyd J, Craig AR, Price CP. *Clin. Chem*., 1997, 43, 109−113.
9. Huang ZZ, Wang HN, Yang WS. *Appl. Mater. Interfaces,* 2015, 7, 8990–8999.
10. Sun HX, Xiang JF, Zhang XF, Chen HB, Yang QF, Li Q, Guan AJ, Shang Q, Tang YL, Xu GZ. *Analyst,* 2014, 139, 581–584.
11. Zeng XD, Ma MS, Zhu BC, Zhu L. *Anal. Sci*., 2016, 32, 1291–1294.
12. Caballero D, Martinez E, Bausells J, Errachid A, Samitier J. *Anal. Chim. Acta,* 2012, 720, 43–48.
13. Tu MC, Chang YZ, Kang YT, Chang HY, Chang P, Yew TR. *Biosens. Bioelectron*., 2012, 34, 286–290.
14. Ermolenko Y, Anshakova A, Osipova N, Kamentsev M, Maksimenko O, Balabanyan V, Gelperina S. *J. Pharmacol. Toxicol. Methods,* 2017, 85, 55–60.
15. Samanta S, Goswami S, Ramesh A, Das G. *J. Photochem. Photobiol. A,* 2015, 310, 45−51.
16. Samanta S, Goswami S, Ramesh A, Das G. *Sens. Actuators, B*, 2014, 194, 120−126.
17. Choudhury R, Parker HE, Cendejas KM, Mendenhall KL. *Tetrahedron Lett*., 2018, 59, 3020-3025.
18. Lord SJ, Lu Z, Wang H, Willets KA, James Schuck P, Lee, HD, Nishimura SY, Twieg RJ, Moerner WE. *J. Phys. Chem. A,* 2007, 111 (37), 8934-8941.
19. Willets KA, Nishimura SY, James Schuck P, Twieg RJ, Moerner WE. *Acc. Chem. Res*., 2005, 38 (7), 549-556.
20. Willets KA, Callis PR, Moerner WE. *J. Phys. Chem. B,* 2004, 108 (29), 10465-10473.
21. Zhong D, Douhal A, Zewail AH. *PNAS*, 2000, 97(26), 14056-14061.
22. Choudhury R, Barman A, Prabhakar R, Ramamurthy V. *J. Phys. Chem. B.,* 2013, 117 (1), 398-407.
23. Kobayashi H, Ogawa M, Alford R, Choyke PL, Urano Y. *Chem. Rev*., 2010, 110 (5), 2620-2640.
24. Staudinger C, Borisov SM. *Methods Appl. Fluoresc*., 2015, 042005.
25. Trott O, Olson AJ. *J. Comput. Chem*., 2009, 31, 455-461.
26. Marini A, Munoz-Losa A, Biancardi A, Mennucci B. *J. Phys. Chem. B*, 2010, 114 (51), 17128-17135.
27. Benesi HA, Hildebrand JH. *J. Am. Chem. Soc*., 1949, 71 (8), 2703-2707.
28. Fujiwara S, Amisaki T. *Biophys. J*., 2008, 94(1), 95-103.